

Zonal Organization of the Vestibulocerebellum in Pigeons (*Columba livia*): II. Projections of the Rotation Zones of the Flocculus

DOUGLAS R.W. WYLIE,^{1,2*} MATTHEW R. BROWN,² RYAN R. BARKLEY,¹
IAN R. WINSHIP,¹ NATHAN A. CROWDER,² AND KATHRYN G. TODD^{2,3}

¹Department of Psychology, University of Alberta, Edmonton, Alberta T6G 2E9, Canada

²Division of Neuroscience, University of Alberta, Edmonton, Alberta T6G 2E9, Canada

³Neurochemical Research Unit, Department of Psychiatry, University of Alberta, Edmonton, Alberta T6G 2E9, Canada

ABSTRACT

Previous neurophysiologic research in birds and mammals has shown that there are two types of Purkinje cells in the flocculus. The first type shows maximal modulation in response to rotational optokinetic stimulation about the vertical axis (*rVA* neurons). The second type shows maximal modulation in response to rotational optokinetic stimulation about a horizontal axis oriented 45 degrees to contralateral azimuth (*rH45c* neurons). In pigeons, the *rVA* and *rH45c* are organized into four alternating parasagittal zones. In this study we investigated the projections of Purkinje cells in the *rVA* and *rH45c* zones by using the anterograde tracers biotinylated dextran amine and cholera toxin subunit B. After iontophoretic injections of tracers into the *rH45c* zones, heavy anterograde labeling was found in the infracerebellar nucleus and the medial margin of the superior vestibular nucleus. Some labeling was also consistently observed in the lateral cerebellar nucleus and the dorsolateral vestibular nucleus. After injections into the *rVA* zones, heavy anterograde labeling was found in the medial and descending vestibular nuclei, the nucleus prepositus hypoglossi, and the central region of the superior vestibular nucleus. Less labeling was seen in the tangential nucleus, the dorsolateral vestibular nucleus, and the lateral vestibular nucleus, pars ventralis. These results are compared and contrasted with findings in mammalian species. *J. Comp. Neurol.* 456:140–153, 2003. © 2002 Wiley-Liss, Inc.

Indexing terms: vestibulocerebellum; optokinetic; Purkinje cells; vestibular nuclei; cerebellar nuclei; anterograde tracer

With respect to the modulation of complex spike activity (CSA) of Purkinje cells in the flocculus by rotational optokinetic stimuli, there are two response types. The first type responds best to rotation about the vertical axis (*rVA* neurons) and the second type responds best to rotation about a horizontal axis oriented 135 degrees to the ipsilateral azimuth and 45 degrees to the contralateral azimuth (*rH45c* neurons). These response types were found first in rabbits (Simpson et al., 1981, 1988, 1989a,b; Graf et al., 1988; see also Leonard et al., 1988) and subsequently in pigeons (Wylie and Frost, 1993; see also Winship and Wylie, 2001). The rabbit flocculus contains two *rVA* zones interdigitated with two *rH45c* zones (De Zeeuw et al., 1994; Tan et al., 1995a). In the companion paper (Winship and Wylie, 2003), we showed that the pigeon

flocculus also has four parasagittal zones: two *rVA* zones are interdigitated with two *rH45c* zones (see Fig. 4).

Grant sponsor: Natural Sciences and Engineering Research Council of Canada; Grant sponsor: Canadian Institute for Health Research; Grant sponsor: Davey Endowment for Brain Injury Research; Grant sponsor: Alberta Heritage Foundation for Medical Research.

*Correspondence to: Douglas R.W. Wylie, Department of Psychology, University of Alberta, Edmonton, Alberta T6G 2E9, Canada.
E-mail: dwylie@ualberta.ca

Received 6 December 2001; Revised 23 July 2002; Accepted 25 September 2002

DOI 10.1002/cne.10508

Published online the week of December 16, 2002 in Wiley InterScience (www.interscience.wiley.com).

De Zeeuw et al. (1994) injected the anterograde tracer biocytin into physiologically identified zones of the rabbit flocculus (see also Tan et al., 1995b). The *rVA* zones projected to the medial vestibular nucleus (VeM) and the prepositus hypoglossi (ph; see Yamamoto, 1978), whereas the *rH45c* zones projected to the superior vestibular nucleus (VeS), the ventral dentate nucleus, and group Y. Previous studies revealed that pigeon flocculus projects to VeM, VeS, ph, the dorsolateral vestibular nucleus (VDL), the lateral cerebellar nucleus (CbL), the cerebellovestibular process (pcv), the descending vestibular nucleus (VeD), the tangential vestibular nucleus (Ta), and the infracerebellar nucleus (Inf; Arends et al., 1991; Wylie et al., 1999a). However, the differential projections of the *rVA* and *rH45c* zones have yet to be investigated in pigeons. In the present study, we used methods similar to those of De Zeeuw et al. (1994) to determine the zonal projection of the pigeon flocculus.

MATERIALS AND METHODS

The methods reported herein conformed to the guidelines established by the Canadian Council on Animal Care and were approved by the Biosciences Animal Care and Policy Committee at the University of Alberta. Other than the site of recording (vestibulocerebellum vs. inferior olive), the methods for anesthesia, surgery, recording, and tissue processing are essentially identical to those described in the companion paper (Winship and Wylie, 2003) and the details are not described in detail here. After the pigeons were placed in a stereotaxic device so that the head conformed to the orientation of the atlas of Karten and Hodos (1967), access to the flocculus was achieved by removing bone surrounding the semicircular canals, but the canals themselves remained intact. The dorsal surface of the flocculus (folium IXcd) lies within the radius of the anterior semicircular canal. The dura was removed, and glass micropipettes, filled with 2 M NaCl and having tip diameters of 4–5 μm , were inserted to record the CSA of Purkinje cells. CSA can be easily identified based on the low firing rate of about 1 spike/second. After a cell was

isolated, the optic flow preference of the CSA was determined by using the methods described in the companion paper (Winship and Wylie, 2003). As was the case for olivary neurons, we found that the most convenient way to identify the flowfield preference was to use computer-generated largefield drifting gratings that were presented to the frontal visual field (from 45 degrees ipsilateral [i] to 45 degrees contralateral [c] azimuth), the contralateral hemifield (from 45 to 135 degrees c azimuth), or the ipsilateral hemifield (from 45 to 135 degrees i azimuth; Fig. 1A).

After identification of the CSA as *rVA* or *rH45c*, the recording electrode was replaced with a pipette (tip diameter, 10–20 μm) containing an anterograde tracer. In one case (RB5) low-salt cholera toxin subunit B (CTB; 1% in 0.1 M phosphate buffered saline [PBS; pH 7.4]; Sigma, St. Louis, MO) was iontophoretically injected for 1.5 minutes (+4 μA , 7 seconds on, 7 seconds off). In all other cases, biotinylated dextran amine (BDA; Molecular Probes, Eugene, OR; 10% in 0.1 M phosphate buffer [PB; pH 7.4]) was iontophoretically injected (+3 μA , 1 second on, 1 second off) for 2 to 5 minutes.

After a survival time of 3 to 5 days, the animals were given an overdose of sodium pentobarbitol (100 mg/kg) and perfused with saline (0.9%) followed by ice-cold paraformaldehyde (4% in 0.1 M PB). The brains were extracted, postfixed for 2–12 hours (4% paraformaldehyde, 20% sucrose in 0.1 M PB), cryoprotected in sucrose overnight (20% in 0.1 M PB), and embedded in gelatin. Frozen sections, 45 μm thick, were collected in the coronal plane. The BDA or CTB was visualized by using a cobalt chloride intensification of diaminobenzidine. These procedures have been described in detail elsewhere (BDA: Wylie et al., 1997; CTB: Lau et al., 1998; see also Wild, 1993; Veenman et al., 1992). The tissue was mounted on gelatin chrome aluminium-coated slides, lightly counterstained with Neutral Red, and examined with light microscopy. In some cases coronal sections were drawn with the aid of a drawing tube. The photomicrographs shown in Figures 2 and 3 were taken with a compound light microscope (Olympus Research Microscope BX60) equipped with a

Abbreviations

An	nucleus angularis	MR	medial rectus
AOS	accessory optic system	nIX	glossopharyngeal nerve
AVT	area ventralis of Tsai	nBOR	nucleus of the basal optic root
BDA	biotinylated dextran amine	NOT	nucleus of the optic tract
CbL	lateral cerebellar nucleus	PCV/pcv	cerebellovestibular process
CbM	medial cerebellar nucleus	PH/ph	nucleus prepositus hypoglossi
CF	climbing fiber	Pl	Purkinje layer
CSA	complex spike activity	rb	restiform body
CTB	cholera toxin subunit B	S	solitary nucleus
dc	dorsal cap	sa	stria acoustica
fl	folium I	SO	superior oblique
gl	granule layer	SR	superior rectus
Inf	infracerebellar nucleus	Ta	tangential nucleus
IO	inferior oblique	VDL	dorsolateral vestibular nucleus
IR	inferior rectus	VDN	ventral dentate nucleus
LM	nucleus lentiformis mesencephali	VeD	descending vestibular nucleus
LR	lateral rectus	VeLd	lateral vestibular nucleus, pars dorsalis
mIII	oculomotor nucleus	VeLv	lateral vestibular nucleus, pars ventralis
mIV	trochlear nuclear	VeM	medial vestibular nucleus
mVI	abducens nucleus	VeS	superior vestibular nucleus
MC	nucleus magnocellularis	vlo	ventrolateral outgrowth
mcIO	medial column of the inferior olive	VTRZ	visual tegmental relay zone
ml	molecular layer		

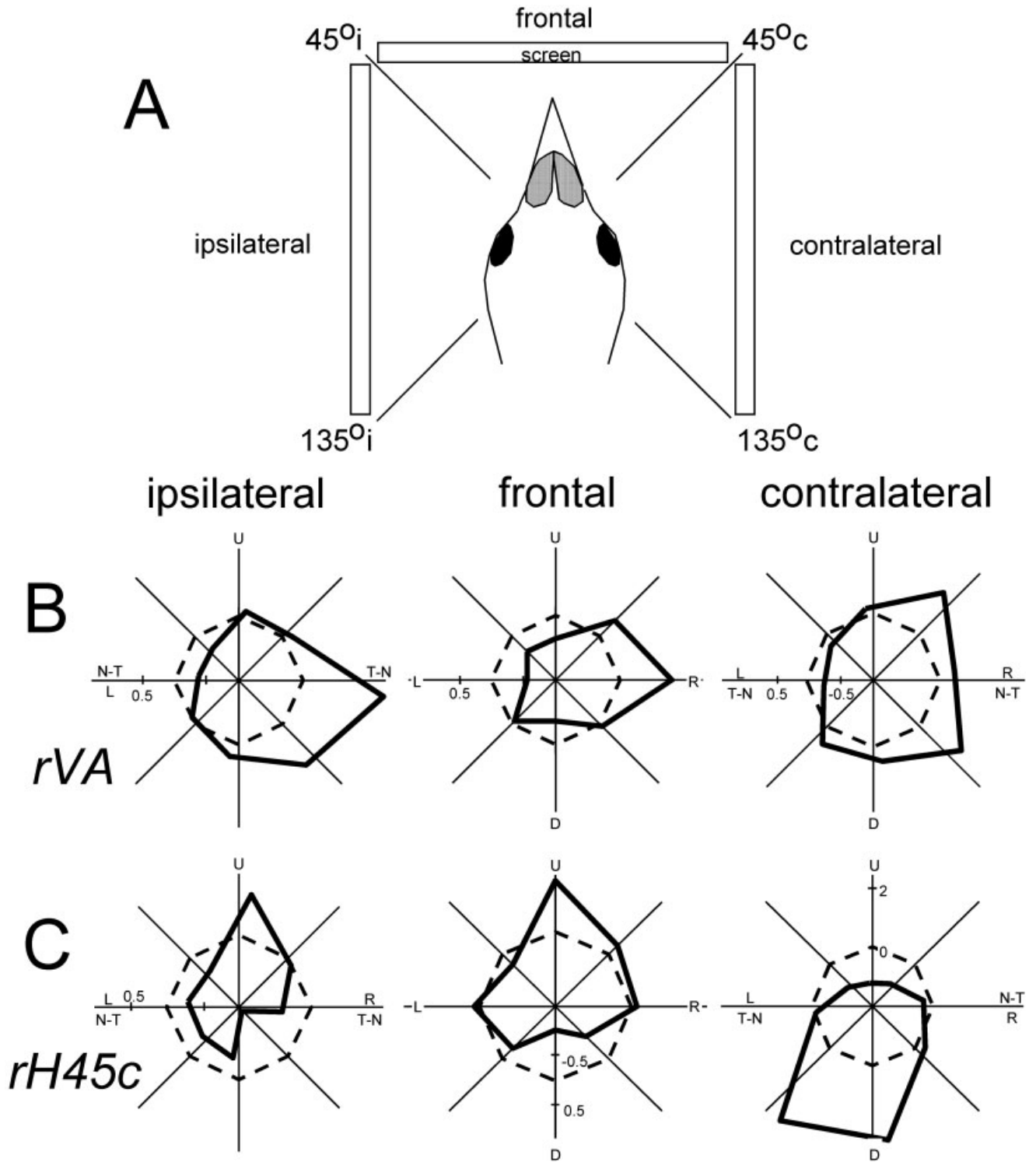


Fig. 1. Directional tuning of complex spike activity of floccular Purkinje cells to moving largefield sine wave gratings presented in different regions of the visual field. Drifting gratings were back projected onto a screen that measured 90 × 75 degrees (width × height). **A:** The screen was positioned at one of three locations relative to the bird: the contralateral, ipsilateral, and frontal regions (recordings were made in the left flocculus). An *rVA* neuron (**B**) and an *rH45c* neuron (**C**) respond to the drifting gratings in each of the three

regions. Polar plots of direction tuning are shown (firing rate, spikes per second with respect to spontaneous rate) as a function of the direction of largefield motion). The broken circles represent the spontaneous rate (set to 0 spikes/second). U, D, L, and R, upward, downward, leftward, and rightward motions, respectively; N-T and T-N, nasal to temporal and temporal to nasal motions, respectively; i, ipsilateral; c, contralateral.

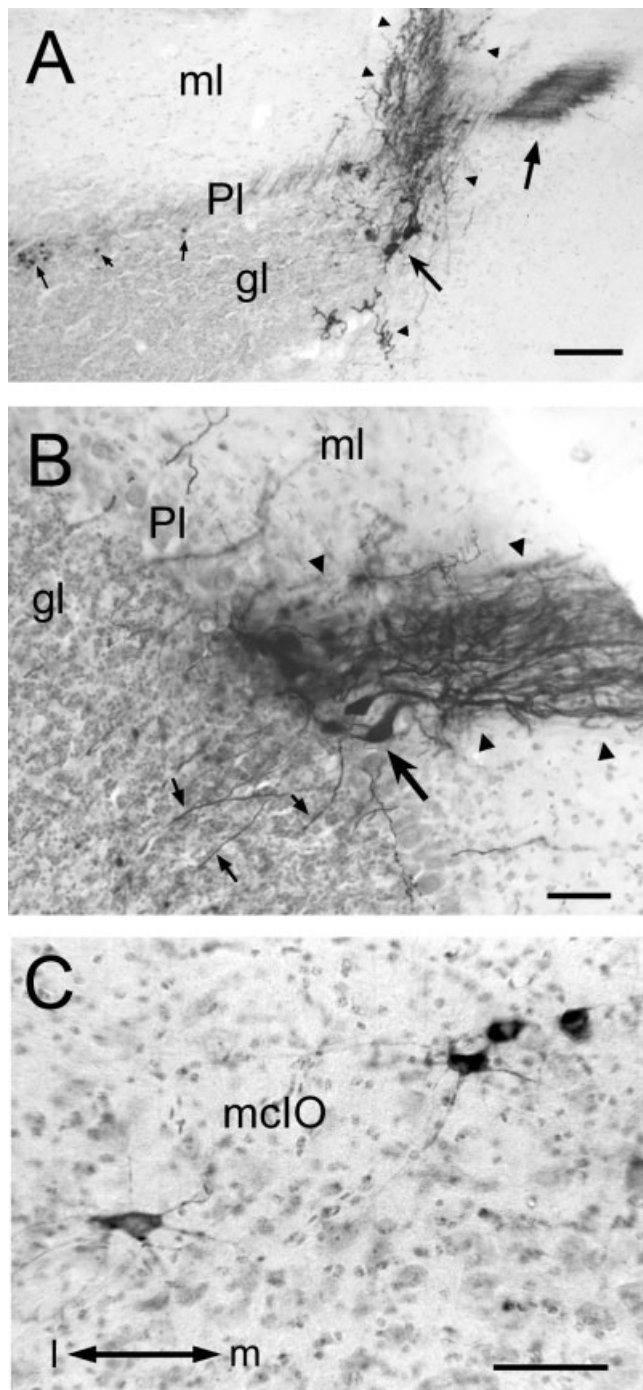


Fig. 2. Photomicrographs of two injection sites in the flocculus. **A:** The injection site was in the dorsal lamella of folium X in the lateral *rVA* zone. **B:** The injection was in the auricle in the lateral *rH45c* zone. Arrowheads indicate labeled Purkinje cell bodies and the triangles indicate labeled Purkinje cell dendrites in the molecular layer (ml). In A, larger arrows indicate the parallel fiber beam and the smaller arrows indicate retrogradely labeled granule cells. **C** shows four retrogradely labeled cells in the medial column of the inferior olive (mcIO) from case RB5, the only case in which cholera toxin was used. Pl, Purkinje layer; gl, granular layer; m, medial; l, lateral. Scale bars—100 μ m in A, 50 μ m in B and C.

digital camera (Media Cybernetics CoolSNAP-Pro color digital camera). Adobe Photoshop software was used to compensate for brightness and contrast.

Nomenclature

For nomenclature related to the description of the different parts of the vestibulocerebellum, see the companion paper (Winship and Wylie, 2003). For the vestibular and cerebellar nuclei, we generally use the nomenclature of Karten and Hodos (1967) with a few exceptions. According to Karten and Hodos (1967), there are two cerebellar nuclei: the medial and lateral cerebellar nuclei (CbM and CbL, respectively), although CbM can be subdivided further. Arends and Zeigler (1991) identified a third nucleus, the infracerebellar nucleus, which is difficult to distinguish. Inf lies ventral and lateral to the rostral part of CbL and dorsal to VDL (see also Labendeira-Garcia et al., 1989; Arends et al., 1991). The indistinct regions between the CbM, CbL, and the vestibular complex are collectively referred to as the cerebellovestibular process (pcv). According to Karten and Hodos (1967), the vestibular nuclear complex consists of the medial vestibular nucleus (VeM), the superior vestibular nucleus (VeS), the descending vestibular nucleus (VeD), the lateral vestibular nucleus, pars dorsalis (VeLd) and pars ventralis (VeLv), and the dorsolateral vestibular nucleus (VDL). Most of the VeM lies dorsal and medial to the stria acoustica, but part of the VeM lies ventral to this fiber bundle. This ventral region of the VeM appears to merge with, and is difficult to distinguish from, the prepositus hypoglossi (ph), which lies ventromedially. In mammals, VeLv is now referred to as the magnocellular VeM (Epema et al., 1988; Ruberstone et al., 1995). Dickman and Fang (1996) considered VDL to be the dorsal extension of VeLv. They also identified groups A and B in pigeons, based on earlier studies in chickens (Wold, 1976; Dickman and Fang, 1996). In our material, we could not reliably identify groups A and B, so they were not included in our analysis. The tangential nucleus (Ta) is a collection of large neurons that lies medially to the root of the vestibular nerve. Arends et al. (1991) suggested that the mammalian homolog of Ta is a group of oculomotor-projecting neurons on border of VeM and VeL (Carleton and Carpenter, 1983; Sato et al., 1987).

RESULTS

Experiments were performed in 14 animals, but data from five cases were discarded. For one of these cases, the CSA modulation was inconclusive. For two of these cases, the injections extended outside the flocculus into folia IXab and VIII. In the other two discarded cases, the injections were confined to the vestibulocerebellum, but were extremely large (width > 1 mm), and most certainly extended across more than one floccular zone and perhaps encroached upon the translation areas of the medial vestibulocerebellum (Wylie et al., 1993, 1998; Wylie and Frost, 1999).

Thus, data from nine cases are described. For these cases the injection sites were quite compact (<300 μ m in width; Table 1) and CSA was reliably recorded and quantitatively identified as the *rVA* or *rH45c* response type. The direction tuning of CSA for an *rVA* neuron and an *rH45c* neuron in response to gratings drifting in the frontal, ipsilateral, and contralateral regions of the visual field are shown in Figure 1B and 1C, respectively. In this

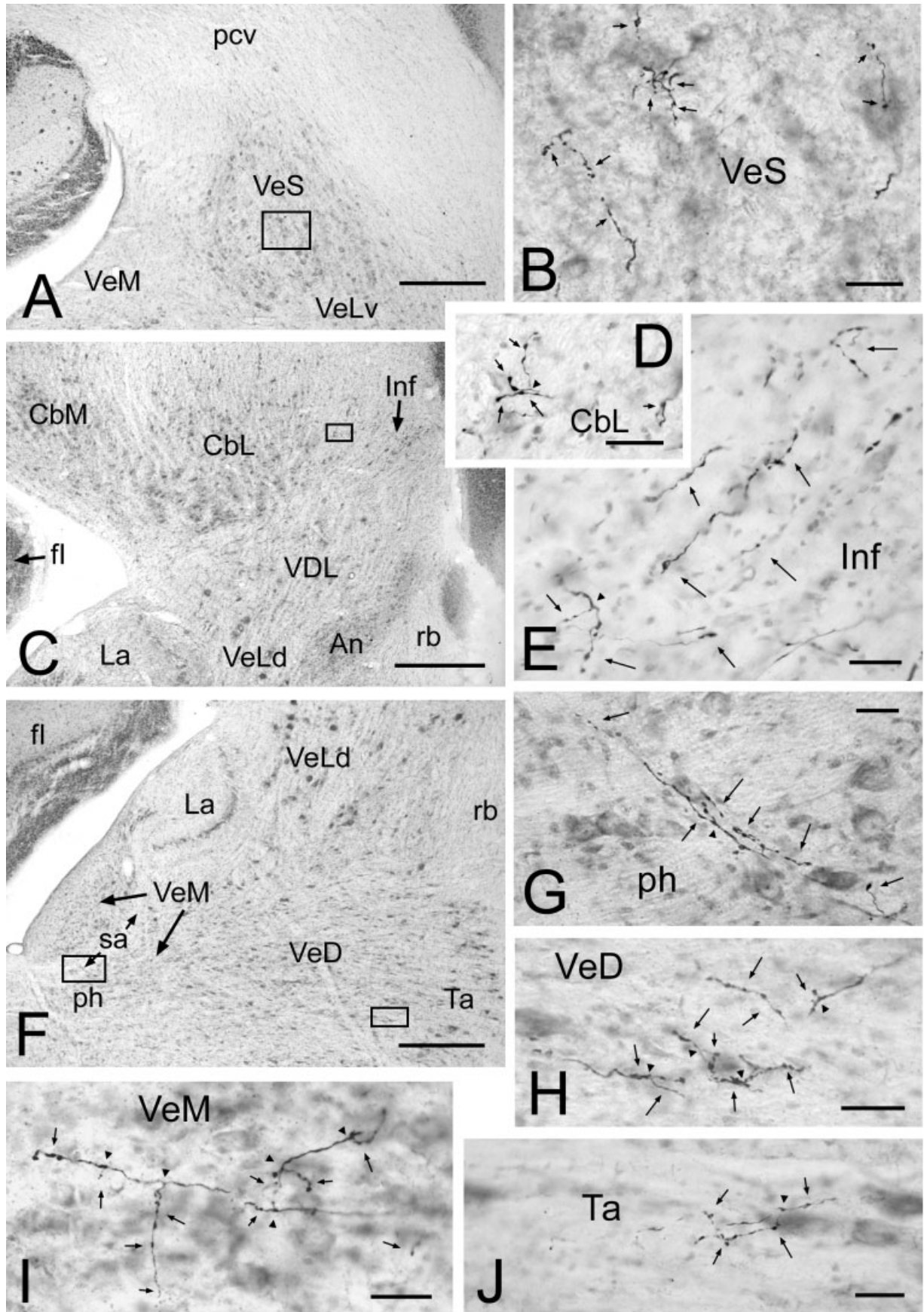


Figure 3

TABLE 1. Zonal Projection of the Pigeon Flocculus¹

Case	Zone	Distance (μm) from midline	Injection width (μm)	No. of P cells	VeLv	VeM	ph	VeD	Ta	pcv	VeS	VDL	Inf	CbL
RB2	Medial rH45c	3,100	300	25	*	*		*		*	***	**	***	**
RB3	Lateral rH45c	3,200	250	20						*	***	**	***	**
RB4	Lateral rH45c	4,200	150	20						*	**	**	***	**
RB5	Lateral rH45c	4,100	250	30	*	*		*		*	***	**	***	**
MB9	Medial rVA	1,600	280	35	*	***	***	***	*	*	**	*		*
MB10	Medial rVA	2,000	120	20	*	***	**	**		*	***	*	*	*
MB15	Medial rVA	1,800	240	30	*	***	***	***	*	*	***	*		*
RB1	Lateral rVA	3,800	130	20		**		***		*	**	*	*	*
RB6	Lateral rVA	3,700	70	15	*	***	**	***	*	*	***	*	*	

¹The distribution of terminal labeling in the vestibular and cerebellar nuclei after injections of anterograde tracer into the rVA or rH45c zones of the pigeon flocculus is indicated. The approximate size and location (zone and distance from midline) of each injection and the distribution of anterograde labeling are shown for each case. The number of asterisks represents the amount of anterograde labeling: ***, heavy; **, moderate; *, sparse to light. Some details of the differential projections of the rVA and rH45c zones are not captured in this table (i.e., the projections to the different regions of VeS and VDL). CbL, lateral cerebellar nucleus; Inf, infracerebellar nucleus; pcv, cerebellar process; ph, prepositus hypoglossi; rH45c, rotation about a horizontal axis oriented 135 degrees to the ipsilateral azimuth and 45 degrees to the contralateral azimuth; rVA, rotation about the vertical axis; Ta, tangential nucleus; VDL, dorsolateral vestibular nucleus; VeD, descending vestibular nucleus; VeLv, lateral vestibular nucleus, pars ventralis; VeM, medial vestibular nucleus; VeS, superior vestibular.

figure, the firing rate (spikes per second relative to the spontaneous rate) is plotted as a function of the direction of motion in polar coordinates (solid line). The rVA neurons were excited in response to largefield stimuli moving forward (temporal to nasal; T-N) and backward (N-T) in the ipsi- and contralateral visual fields, respectively, and rightward motion in the frontal visual field (for neurons in the left flocculus). The rH45c neurons were excited in response to largefield stimuli moving upward in the ipsilateral and frontal visual fields and downward motion in the contralateral visual field.

Figure 2A,B shows photomicrographs of two injection sites. All injections were into the molecular layer. The cells bodies (arrowheads) and dendritic trees (triangles) of a cluster of 15–30 Purkinje cells were labeled with each injection: up to six Purkinje cells could be seen in one coronal section. A beam of labeled parallel fibers (large arrows) that traversed the folium intersecting the dendritic tree was also labeled. Retrogradely labeled granule cells were also observed scattered throughout the injected folium (small arrows in Fig. 2A). For the CTB injection (case RB5) but none of the BDA injections, retrogradely

labeled cell bodies were also seen in the medial column of the contralateral inferior olive (mcIO; Fig. 2C). About 15–25 cells were seen in the mcIO and all were located dorsomedially within the caudal half of the mcIO. Previous studies showed that this region of the mcIO contains cells rVA cells (Winship and Wylie, 2001) and are retrogradely labeled after injections into the rVA-responsive regions of the flocculus (Wylie et al., 1999b). This pattern of labeling is also consistent with the conclusions of the companion paper (Winship and Wylie, 2003).

There was extensive anterograde terminal labeling (terminal varicosities) in the cerebellar and vestibular nuclei: examples are shown in Figure 3. Figure 3A,B shows terminal labeling in the central VeS from an injection in an rVA zone. Figure 3C,D shows a terminal field located in the lateral CbL, and Figure 3E shows extensive terminal labeling in Inf. These were from injections into rH45c zones. Figure 3G and 3H show terminal fields in the ph and VeD, respectively, from the same coronal section (Fig. 3F). Figure 3I and 3J show labeling in the VeM and Ta, respectively. Figure 3F–J show from cases in which the injections were into the rVA zones.

Figure 4 shows the locations of the injection sites from all nine cases. These are collapsed onto the summary figure from the companion paper (Winship and Wylie, 2003) showing the boundaries of the rVA and rH45c zones. There were four injection sites where we recorded rH45c CSA and five injection sites where we recorded rVA CSA. Of the rVA injection sites, three were in the medial zone, and two were in the lateral zone. Of the rH45c injection sites, three were in the lateral zone and the other was in the medial zone. There was a clear difference with respect to the pattern of anterograde labeling from injections into the rVA and rH45c zones.

Figure 5 shows drawings of coronal sections (approximately 220 μm apart) through the vestibular and cerebellar nuclei from case RB4. The dots indicate the locations of terminals observed in five consecutive coronal sections, collapsed onto the central section. The injection site was

Fig. 3. Photomicrographs showing anterograde labeling in vestibular and cerebellar nuclei. **B** shows terminal labeling among large neurons in the central region of superior vestibular nucleus (VeS) from an injection in an rVA zone. The area in **B** is indicated by the rectangle in **A**. **D** shows a terminal field in the lateral margin of the lateral cerebellar nucleus (CbL), as indicated by the corresponding rectangle in **C**. **E** shows extensive terminal labeling in the infracerebellar nucleus (Inf) from the adjacent section. **B–D** are from injections into an rH45c zone. **G** and **H** show terminal fields in the nucleus prepositus hypoglossi (ph) and the descending vestibular nucleus (VeD), respectively, from the same coronal section (rectangles in **F**). **I** and **J** show labeling in the medial vestibular nucleus (VeM) and the tangential nucleus (Ta), respectively. **F–J** are from cases in which the injections were into rVA zones. The small arrows indicate terminal varicosities and the triangles highlight clear branch points. See list for other abbreviations. Scale bars = 500 μm in A, C, F, 30 μm in B, D, E, G–J.

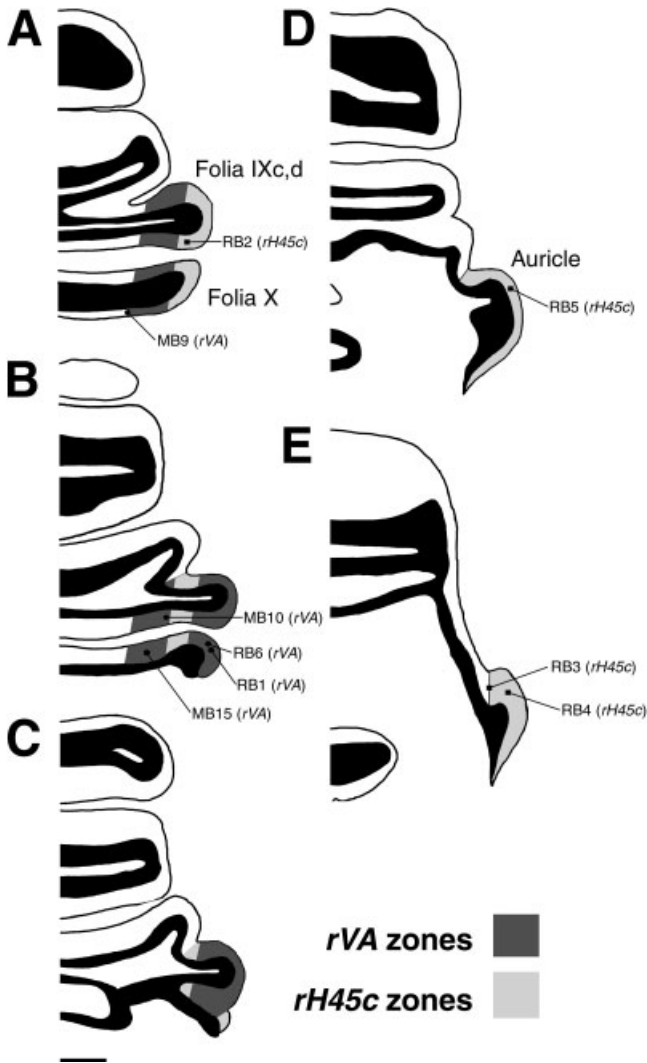


Fig. 4. **A–E:** Locations of the *rVA* and *rH45c* injection sites in the flocculus. This series of drawings shows coronal sections (caudal to rostral; approximately 440 μm apart) through the flocculus to indicate the locations of the four floccular zones. This series is based on data from the companion paper (Winship and Wylie, 2003). The locations of the centers of the nine injection sites are indicated. Scale bar = 1 mm.

located in the lateral *rH45c* zone in the auricle (Fig. 5G,H). The labeled Purkinje cell axons descended, and extremely heavy terminal labeling was observed in Inf (Fig. 5E,F). Labeling was also seen in the most ventral and lateral margins of CbL (Fig. 5D–G). A bundle of the fibers continued medially, and axon collaterals and terminals were observed in an area ventral to the CbL and medial to Inf. Some of these terminals appeared within the borders of VDL, in the dorsomedial region (Fig. 5E,F), whereas others were clearly dorsal and medial to VDL (Fig. 5E–G) but could not be described within any distinctive nucleus. Some fibers continued rostrally and heavy labeling was seen among the large neurons in the medial part of VeS (Fig. 5H–K).

As seen in Table 1, the pattern of anterograde labeling from injections into the *rH45c* zones was strikingly simi-

lar across all four cases. Heavy labeling was always observed in the Inf and moderate to heavy labeling was always observed in the medial VeS. Moderate labeling was always found in the ventrolateral CbL and the dorsomedial margin of VDL. In two cases (RB2 and RB5) a few terminals were also found in the VeM, VeD, and VeLv. We believe that this labeling may be due to encroachment of the injections on adjacent *rVA* zones (see below and Discussion). For the case involving the medial *rH45c* zone (case RB2), there was no apparent difference in the pattern of labeling compared with the three cases that had injections in the lateral zone.

Figure 6 shows drawings of coronal sections (approximately 220 μm apart) through the vestibular and cerebellar nuclei from case RB6. The injection site was in the lateral *rVA* zone in the dorsal lamella of folium X (Fig. 6B,C). Moderate to heavy terminal labeling was seen in VeM (Fig. 6D–K), PH (Fig. 6D–J), VeD (Fig. 6A–H), and VeS (Fig. 6G–K). The terminal labeling in VeM was concentrated in the ventral part of the nucleus on either side of the stria acoustica, which bisects the nucleus (see Fig. 3F). The labeling in VeD was found throughout the nucleus, although concentrated ventrally. Much labeling was seen in the lateral VeD immediately adjacent to Ta, and a moderate amount of terminal labeling was seen in the medial margin of Ta (Fig. 6F,G). The labeling in the VeS was concentrated centrally (Fig. 6I–K). Terminal labeling was not seen in the medial VeS, as was the case with the *rH45c* injections. Some terminal labeling was also seen in VDL (Fig. 6F,G) and VeLv (Fig. 6H,I), and a few terminals were seen in or near Inf (Fig. 6G).

As seen in Table 1, the pattern of anterograde labeling from the *rVA* injections was strikingly similar across all five cases. Moderate to heavy labeling was always seen in VeM, VeD, and the central VeS. In all but one case, moderate to heavy labeling was seen in PH. Labeling was found medially in the Ta in only three cases. (The heaviest labeling in Ta was from case RB6, shown in Fig. 6.) However, in all cases there was moderate to heavy labeling in the lateral VeD, on the border with Ta. In four of the five cases there was some labeling in VeLv and VDL. Most of the labeling in VDL was found in the ventrolateral region, not in the dorsomedial region, as was the case with the *rH45c* injections. In all cases, a few terminals were observed in CbL and Inf, although this labeling could have been due to encroachment of the injections on adjacent *rH45c* zones. There was no apparent difference in the pattern of labeling resulting from the *rVA* cases involving the lateral versus the medial zone.

With respect to case RB5, in which CTB was used, some of the terminal labeling may have been due to the collaterals of retrogradely labeled climbing fiber (CF) axons (Chen and Aston-Jones, 1995). However, the pattern of terminal labeling from this case was not different from those of the other *rVA* cases (Table 1). Also, because in mammals some olivocerebellar fibers branch and innervate the the flocculus and nodulus/uvula (Takeda and Maekawa, 1989a,b), we examined the extent of folia IXcd and X in case RB5 for the presence of retrogradely labeled CF terminals. None was seen.

DISCUSSION

In the present study we injected anterograde tracers into physiologically identified zones of the flocculus in

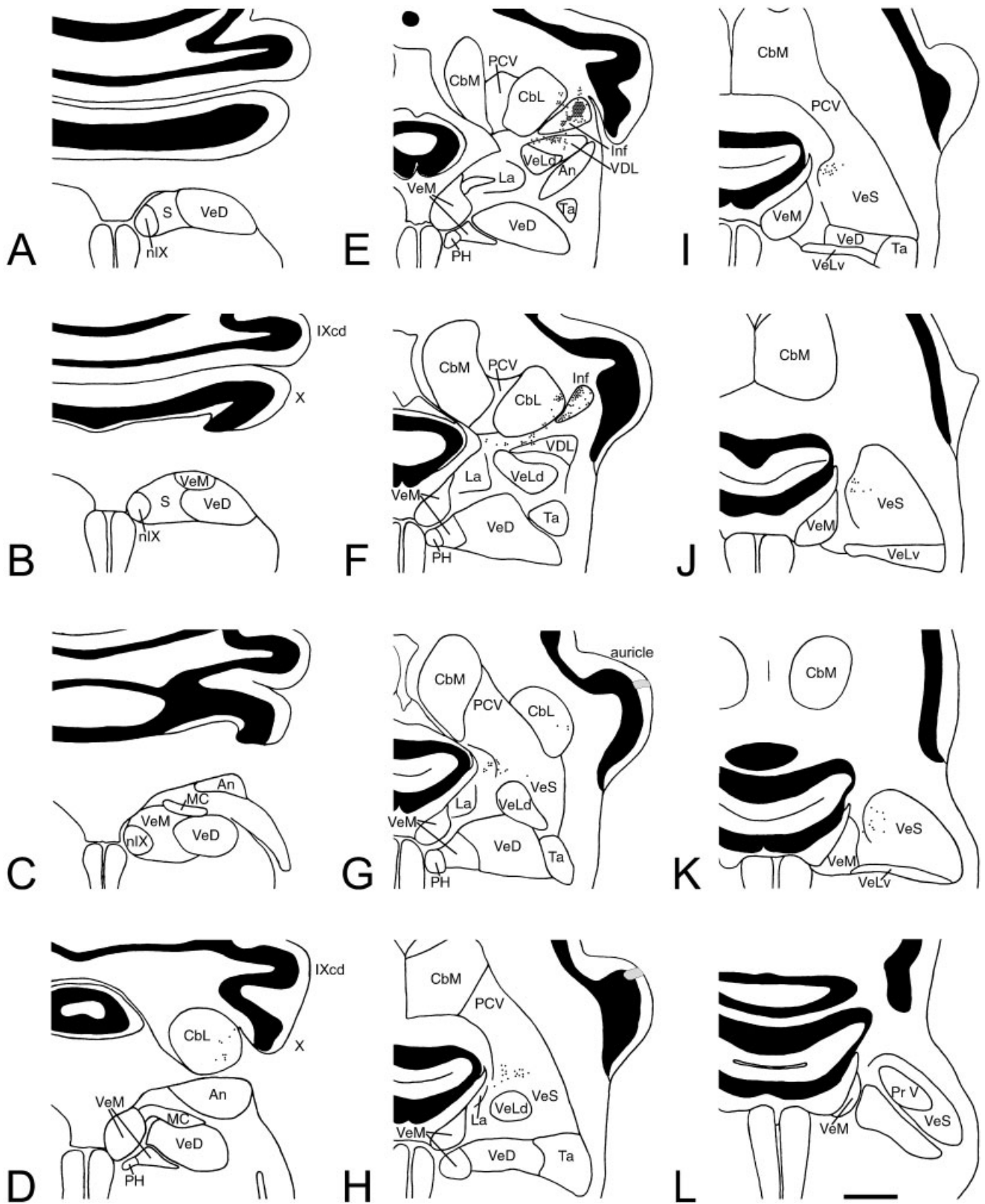


Fig. 5. **A-L:** Projections of the Purkinje cells in the *rH45c* zones. Drawings of coronal sections (caudal, A, to rostral, L; each about 220 μ m apart) from case RB4 are shown. The injection was located in the lateral *rH45c* zone (shaded gray area in G and H). The dots and

stippling indicate the locations of terminals observed in five consecutive sections, collapsed onto the central section. See list for abbreviations. Scale bar = 1 mm.

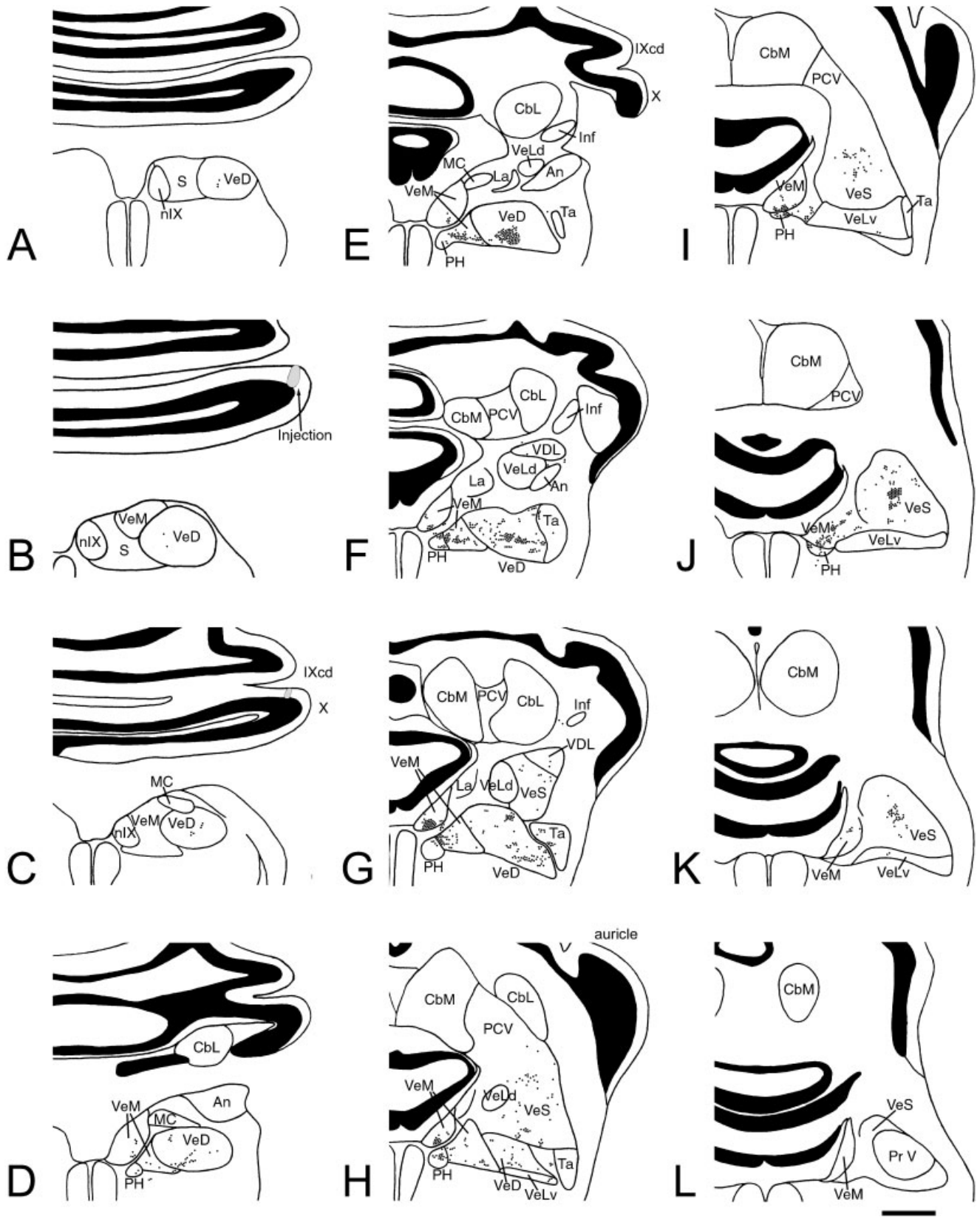


Fig. 6. A-L: Projections of the Purkinje cells in the *rVA* zones. Drawings of coronal sections (caudal, A, to rostral, L; each about 220 μ m apart) from case RB6 are shown. The injection was located in the lateral *rVA* zone (shaded gray area in B and C). The dots and stippling

indicate the locations of terminals observed in five consecutive sections, collapsed onto the central section. See list for abbreviations. Scale bar = 1 mm.

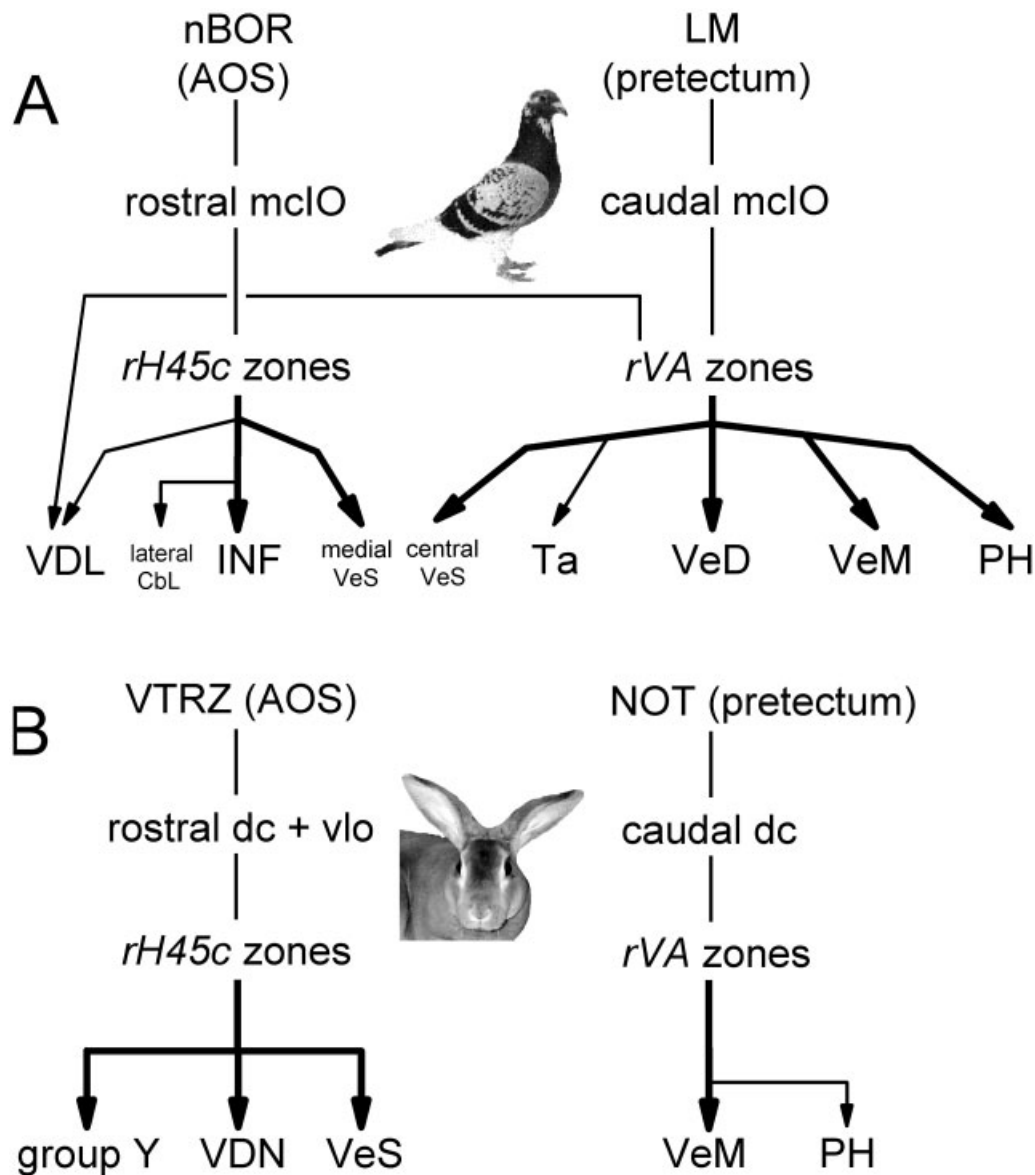


Fig. 7. Organization of the optokinetic olivocerebellar pathways and projections of the floccular zones in pigeons (A) and rabbits (B). The projections from the pretectum and accessory optic system through the subdivisions of the inferior olive to the rVA and rH45c

zones in the flocculus are shown. The projections of the floccular zones to the vestibular and cerebellar nuclei are also shown. See list for abbreviations.

pigeons. Consistent with previous studies, we observed moderate to heavy terminal labeling in VeM, VeD, VeS, ph, and VDL and some labeling in CbL, Ta, the pcv abutting on the CbL/VeS, and VeLv (Arends et al., 1991; Wylie et al., 1999a). Moreover, as summarized in Figure 7, a clear difference in the projection of rVA and rH45c zones was revealed. From injections into the rH45c zones, terminal labeling was extremely heavy in Inf, heavy in the medial VeS, and moderate in the dorsomedial VDL and the lateral edge of CbL. From injections into rVA zones, moderate to heavy terminal labeling was observed in VeM, VeD, ph, and the central VeS. Less labeling was seen in Ta, the ventrolateral VDL, and VeLv. There was

also labeling in VeLv from rVA injections but it was considered too sparse to include in the summary figure.

The data were very consistent with this scheme, with few exceptions. In two rH45c cases a few terminals were seen in VeD and VeM, which may have been due to encroachment of the injection site on adjacent rVA zones. These two cases were large (250 and 300 μm wide). Similarly, the sparse labeling seen in the Inf and CbL from the rVA injections might have been due to spread to adjacent rH45c zones, although some of these injections were quite small. De Zeeuw et al. (1994), in a study of the zonal projection of the flocculus in rabbits (discussed in detail below), confirmed whether an injection was localized to a

particular zone by counterstaining a few sections through the flocculus with acetylcholinesterase, which reveals bands in the floccular white matter of rabbits that contain Purkinje cells axons from a particular zone (see also Tan et al., 1995a). In the present study we had no such assistance. In previous attempts with acetylcholinesterase in pigeons, we did not observe banding in the white matter.

The amount of labeling that we observed in Ta was less than that reported by Arends et al. (1991). They made large injections of wheat germ agglutinin–horseradish peroxidase into the flocculus, which resulted in heavy anterograde labeling in the medial Ta. Large injections centered on Ta resulted in retrogradely labeled Purkinje cells in two distinct zones in the flocculus. Given the findings of the present study, these were likely the two *rVA* zones. We observed terminals actually within Ta from only three of the five *rVA* cases, but moderate to heavy terminal labeling was always found in the lateral VeD, on the border with the medial Ta. It should be noted that the borders between VeD, VeL, and Ta are indistinct.

Terminals were observed in VDL from *rVA* and *rH45c* injections. However, the terminals were concentrated in different regions. From the *rVA* injections, a small amount of terminal labeling was always found in the ventrolateral VDL, from a fiber bundle that coursed ventrally and entered the VeS, or entered the lateral VeD and provided input to the VeD and Ta. From the *rH45c* injections, a more substantial amount of terminal labeling was seen in the dorsolateral VDL, from a fiber bundle that traveled medially from Inf and continued to the medial VeS.

Moderate to heavy labeling was observed in VeS from *rVA* and *rH45c* injections, but the labeling was localized to the central and medial regions, respectively. This is remarkably consistent with the primary vestibular projection to VeS in pigeons. Dickman and Fang (1996) found a differential projection to VeS from the semicircular canals. The vertical and horizontal canals projected to the medial and central regions of VeS, respectively.

Comparison with the zonal projection of the rabbit flocculus

Figure 7 outlines the afferent CF input and the efferent connections of the *rVA* and *rH45c* floccular zones in pigeons (Fig. 7A) and rabbits (Fig. 7B). Previous studies have shown that the CF inputs and the visual inputs from the accessory optic system (AOS) and pretectum to the inferior olive are remarkably similar. In pigeons, the *rVA* and *rH45c* zones receive CF input from the caudal and rostral halves of the mcIO, respectively (Wylie et al., 1999b; see also Winship and Wylie, 2003). Similarly, there is a rostrocaudal organization of the CF inputs in rabbits: the *rVA* zones received CF input from the caudal dorsal cap, whereas the *rH45c* zones received CF input from the rostral dorsal cap and ventrolateral outgrowth (Leonard et al., 1988; Ruigrok et al., 1992; Tan et al., 1995a). Most of the visual input to the caudal mcIO in pigeons originated in the nucleus lentiformis mesencephali of the pretectum (Wylie, 2001). Likewise, in rabbits the visual input to the caudal dorsal cap arises from the homologous pretectal structure, the nucleus of the optic tract (Mizuno et al., 1973; Takeda and Maekawa, 1976; Maekawa and Takeda, 1977; Holstege and Collewijn, 1982). The bulk of the visual input to the rostral mcIO in pigeons originates in the nucleus of the basal optic root (nBOR) of the AOS. The nBOR projects to directly to the rostral mcIO, but also

indirectly, via the area ventralis of Tsai in the ventral tegmentum (Brecha et al., 1980; Wylie, 2001). In rabbits, most of the visual input to the rostral dorsal cap and ventrolateral outgrowth arises from the medial and lateral terminal nuclei of the AOS via the visual tegmental relay zone in the ventral tegmentum (Maekawa and Takeda, 1979; Simpson, 1984; Giolli et al., 1985; Blanks et al., 1995). In summary, studies have shown that the optokinetic olivocerebellar pathways to the flocculus are highly conserved.

Although these CF pathways to the vestibulocerebellum seem highly conserved, there is also a direct mossy fiber pathway from the nBOR and pretectum to the vestibulocerebellum in pigeons (Clarke, 1977; Brecha et al., 1980; Wylie et al., 1997). The mossy fiber pathway from the AOS to the vestibulocerebellum has also been reported in fish (Finger and Karten, 1978) and turtles (Reiner and Karten, 1978) but not in frogs (Montgomery et al., 1981). In mammals, this pathway has been reported in the chinchilla (Winfield et al., 1978), but is absent in cats (Kawasaki and Sato, 1980), rats, and rabbits (Giolli et al., 1984).

From Figure 7, it appears that there are some differences between pigeons and rabbits with respect to the projections of the *rVA* and *rH45c* zones. The zonal projection of the rabbit flocculus is quite straightforward. The *rVA* zones in rabbits project to VeM and to ph (De Zeeuw et al., 1994), although this latter projection is weaker and may be restricted to Purkinje cells in folium p (Yamamoto, 1978). The *rH45c* zones project to VeS, group Y, and the ventral dentate nucleus (De Zeeuw et al., 1994). Strikingly similar projection patterns exist in pigeons. The *rVA* zones project to VeM and ph, although the latter projection appears to be stronger in pigeons than in rabbits. As in rabbits, the *rH45c* zones project to VeS. In pigeons, this projection is restricted to the medial VeS and, unlike rabbits, the *rVA* zones project to the central VeS. The heaviest projection of the pigeon *rH45c* zones is to Inf. Based on the fact that Inf provides a heavy input to oculomotor structures, it has been suggested that Inf is homologous to group Y, in particular the dorsal subgroup (Arends et al., 1991; see also Labandeira-Garcia et al., 1989; for a review of the mammalian anatomy, see Highstein and McCrea, 1988). Arends et al. (1991) also suggested that VDL could be considered homologous to ventral group Y, although they noted that the evidence is less compelling. In rabbits, the projection of the *rH45c* zones to group Y is heavier to the dorsal subgroup than to the ventral subgroup (De Zeeuw et al., 1994). In parallel, the projection of the pigeon *rH45c* zones is heavier to Inf than to VDL. The projections of the pigeon *rVA* zones to VeD, central VeS, Ta, and VDL in pigeons are not found in rabbits. Also, the projection of the pigeon *rH45c* zones to the lateral part of CbL in pigeons is not found in rabbits. CbL corresponds to the mammalian interposed nucleus. The posterior interposed nucleus does receive input from the flocculus, but from the nonvisual C2 zone rather than from the *rH45c* zones (De Zeeuw et al., 1994).

Connections with collimator and oculomotor structures

Arends et al. (1991) examined the projections of the vestibular nuclei to oculomotor and collimator structures. The pigeon flocculus projects to some structures that are largely collimator (VDL) or oculomotor (Inf) and to some structures that feed the oculomotor and collimator sys-

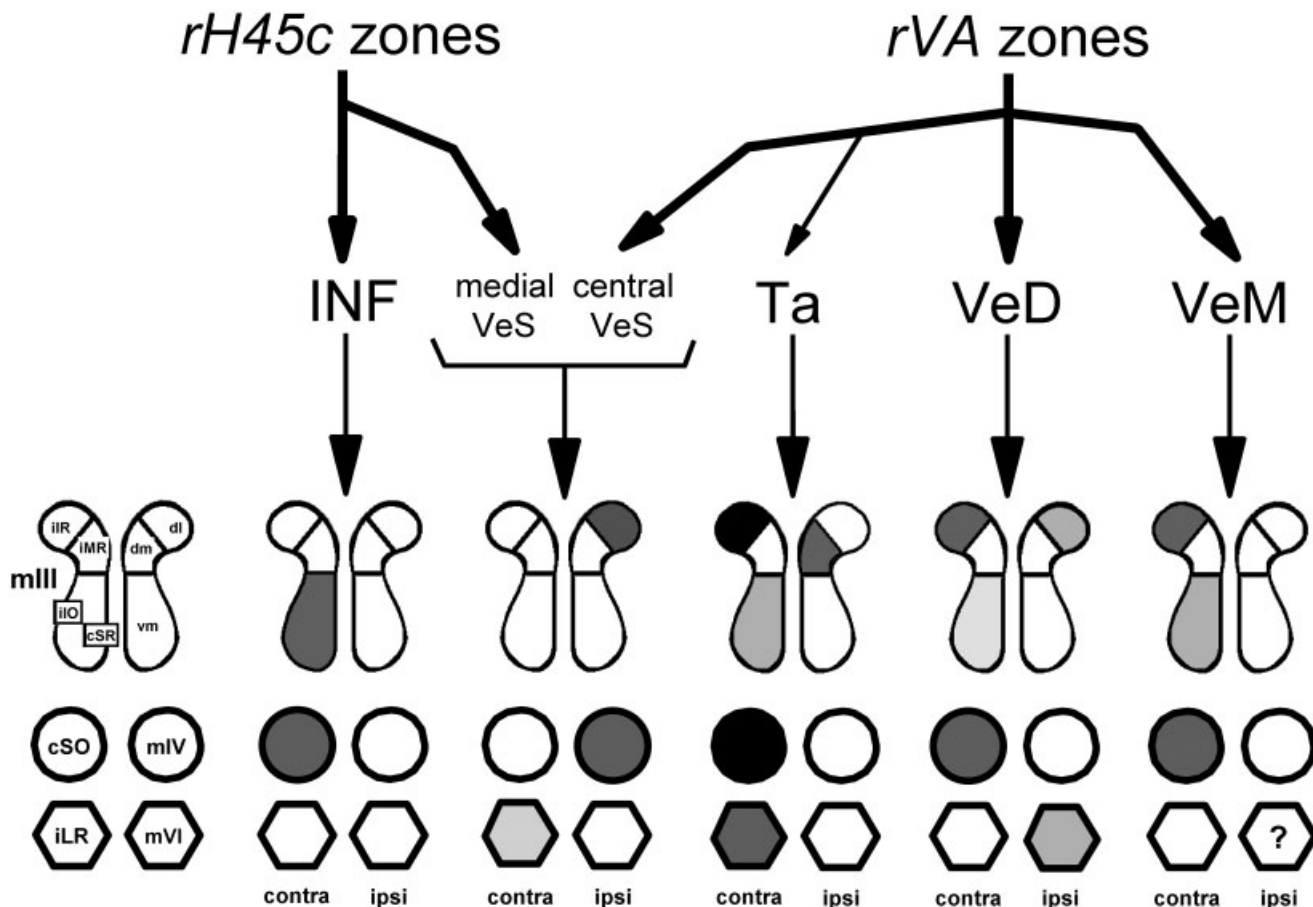


Fig. 8. Association of the flocculus zones with oculomotor nuclei in pigeons. The projections of the *rVA* and *rH45c* zones to vestibular nuclei that project to the oculomotor nuclei are shown. In turn, the projections of the vestibular nuclei to the ipsilateral (i; left) and contralateral (c; right) projections to the oculomotor nuclei are shown. These include the trochlear (mIV; circle) and abducens (mVI; hexagon) nuclei and the dorsolateral (dl), dorsomedial (dm), and ventro-

medial (vm) regions of the oculomotor nuclei (mIII). On the far left, the innervation of the extraocular muscles by mIV, mVI, and the subdivisions of mIII are shown. The shading in mIV, mVI, and the subdivision of mIII indicate the strength of the afferent input from the vestibular nuclei (darker = stronger) based on data from Arends et al. (1991). See list for abbreviations.

tems (Ta, VeD, VeM, and VeS). Although the connections have not been shown in pigeons, studies in mammals have shown that the ph is also important for oculomotor functions (for review, see McCrea, 1988).

Figure 8 shows the projections of the floccular zones to structures that provide input to the oculomotor nuclei in pigeons. The afferent connections of the oculomotor, trochlear, and abducens nuclei (mIII, mIV, and mVI, respectively) are based on a comprehensive summary by Arends et al. (1991). De Zeeuw et al. (1994) summarized how the *rVA* and *rH45c* floccular zones in rabbits are associated with preoculomotor structures controlling the horizontal recti, the obliques, and vertical recti, respectively. One would expect the same pattern in pigeons. For the *rH45c* zones this seems to be the case. Inf projects contralaterally to mIV and the ventromedial region of mIII (mIII-vm), which controls the superior muscles and the inferior oblique. The pattern of connectivity of the oculomotor nuclei with the extraocular muscles in birds is virtually identical to that in mammals (Heaton and Wayne, 1983). The heaviest oculomotor projections of VeS are to the

dorsolateral regions of mIII (mIII-dl) and mIV, which control the superior oblique and inferior rectus.

Unlike the situation in rabbits, the pigeon *rVA* zones do not project exclusively to the dorsomedial region of mIII (mIII-dm) and mVI, structures that control the medial and lateral recti. Ta does provide substantial input to mIII-dm and mVI, but Ta provides heavier inputs to mIII-dl and mIV and a weaker input to mIII-vm. Similarly, VeD projects to mVI, but inputs to mIII-dl, mIV, and mIII-vm are of equal or greater strength. VeM also provides robust inputs to mIII-dl and mIV and a weaker input to mIII-vm. Arends et al. (1991) were unable to determine whether VeM and ph project to mVI (because of proximity), although in mammals VeM and ph are major sources of afferent input to mVI (Highstein and McCrea, 1988; McCrea, 1988). VeS is a source of a weak input to mVI, but it is not known whether this originates in the central VeS.

The fact that the pigeon *rVA* zones do not project exclusively to preoculomotor structures controlling the horizontal recti, as is the case in rabbit, may be explained by the

peculiar arrangement of these muscles. Wylie and Frost (1996) showed that, although the orientation of the medial rectus is in the horizontal plane, the lateral rectus is not. In fact, the lateral rectus is oriented such that its action would rotate the eye laterally and downward about an axis that is about 20 degrees off the vertical. Thus, an abduction of the eye requires a synergistic effort by the lateral rectus, the obliques, and vertical recti. For example, a leftward head rotation about the vertical axis would induce rightward optic flow, which would maximally excite CSA in the *rVA* zones in the left flocculus. The appropriate compensatory eye movement would be adduction and abduction of the left and right eyes, respectively. Adduction of the left eye would be accomplished (largely) by contraction of the medial rectus. Abduction of the right eye would require action of the other extraocular muscles in addition to contraction of the lateral rectus.

LITERATURE CITED

- Arends JJA, Zeigler HP. 1991. Organization of the cerebellum in the pigeon (*Columba livia*): I. Corticonuclear and corticovestibular connections. *J Comp Neurol* 306:221–244.
- Arends JJA, Allen RW, Zeigler HP. 1991. Organization of the cerebellum in the pigeon (*Columba livia*): III. Corticovestibular connections with eye and neck premotor areas. *J Comp Neurol* 306:273–289.
- Blanks RH, Clarke RJ, Lui F, Giolli FA, Van Pham S, Torigoe Y. 1995. Projections of the lateral terminal accessory optic nucleus of the common marmoset (*Callithrix jacchus*). *J Comp Neurol* 354:511–532.
- Brecha N, Karten HJ, Hunt SP. 1980. Projections of the nucleus of basal optic root in the pigeon: an autoradiographic and horseradish peroxidase study. *J Comp Neurol* 189:615–670.
- Carleton SC, Carpenter MB. 1983. Afferent and efferent connections of the medial, inferior and lateral vestibular nuclei in the cat and monkey. *Brain Res* 278:29–51.
- Chen S, Aston-Jones G. 1995. Evidence that cholera toxin B subunit (CTb) can be avidly taken up and transported by fibers of passage. *Brain Res* 674:107–111.
- Clarke PGH. 1977. Some visual and other connections to the cerebellum of the pigeon. *J Comp Neurol* 174:535–552.
- De Zeeuw CI, Wylie DR, DiGiorgi PL, Simpson JI. 1994. Projections of individual Purkinje cells of physiologically identified zones in the flocculus to the vestibular and cerebellar nuclei in the rabbit. *J Comp Neurol* 349:428–447.
- Dickman JD, Fang Q. 1996. Differential central projections of vestibular afferents in pigeons. *J Comp Neurol* 367:110–131.
- Epema AH, Gerrits NM, Voogd J. 1988. Commissural and intrinsic connections of the vestibular nuclei in the rabbit: a retrograde labelling study. *Exp Brain Res* 71:129–146.
- Finger TE, Karten HJ. 1978. The accessory optic system in teleosts. *Brain Res* 153:144–149.
- Giolli RA, Blanks RHI, Torigoe Y. 1984. Pretectal and brain stem projections of the medial terminal nucleus of the accessory optic system of the rabbit and rat as studied by anterograde and retrograde neuronal tracing methods. *J Comp Neurol* 232:91–116.
- Giolli RA, Blanks RHI, Torigoe Y, Williams DD. 1985. Projections of the medial terminal nucleus, ventral tegmental nuclei and substantia nigra of rabbit and rat as studied by retrograde axonal transport of horseradish peroxidase. *J Comp Neurol* 227:228–251.
- Graf W, Simpson JI, Leonard CS. 1988. Spatial organization of visual messages of the rabbit's cerebellar flocculus. II. Complex and simple spike responses of Purkinje cells. *J Neurophysiol* 60:2091–2121.
- Heaton MB, Wayne DB. 1983. Patterns of extraocular innervation by the oculomotor complex in the chick. *J Comp Neurol* 216:245–252.
- Highstein SM, McCrea RA. 1988. The anatomy of the vestibular nuclei. In: Buettner-Ennever J, editor. *Neuroanatomy of the oculomotor system*. New York: Elsevier. p 177–202.
- Holstege G, Collewijn H. 1982. The efferent connections of the nucleus of the optic tract and the superior colliculus in rabbit. *J Comp Neurol* 209:139–175.
- Karten HJ, Hodos W. 1967. A stereotaxic atlas of the brain of the pigeon (*Columba livia*). Baltimore: Johns Hopkins Press.
- Kawasaki T, Sato Y. 1980. Afferent projection from the dorsal nucleus of the raphe to the flocculus in cats. *Brain Res* 197:496–502.
- Labendeira-Garcia JL, Guerra-Seijas MJ, Labendeira-Garcia JA, Jorge-Barreiro FJ. 1989. Afferent connections of the oculomotor nucleus in the chick. *J Comp Neurol* 259:140–149.
- Lau KL, Glover RG, Linkenhoker B, Wylie DRW. Topographical organization of inferior olive cells projecting to translation and rotation zones in the vestibulocerebellum of pigeons. *Neurosci* 85:605–614.
- Leonard CS, Simpson JI, Graf W. 1988. Spatial organization of visual messages of the rabbit's cerebellar flocculus. I. Typology of inferior olive neurons of the dorsal cap of Kooy. *J Neurophysiol* 60:2073–2090.
- Maekawa K, Takeda T. 1977. Afferent pathways from the visual system to the cerebellar flocculus of the rabbit. In: Baker R, Berthoz A, editors. *Control of gaze by brain stem neurons. Developments in neuroscience. Volume 1*. Amsterdam: Elsevier. p 187–195.
- Maekawa K, Takeda T. 1979. Origin of descending afferents to the rostral part of the dorsal cap of the inferior olive which transfers contralateral optic activities to the flocculus. A horseradish peroxidase study. *Brain Res* 172:393–405.
- McCrea RA. 1988. The nucleus prepositus. In: Buettner-Ennever J, editor. *Neuroanatomy of the oculomotor system*. New York: Elsevier. p 203–221. 2
- Mizuno N, Mochizuki K, Akimoto C, Matsushima R. 1973. Pretectal projections to the inferior olive in the rabbit. *Exp Neurol* 39:498–506.
- Montgomery N, Fite KV, Bengston L. 1981. The accessory optic system of *Rana pipiens*: neuroanatomical connections and intrinsic organization. *J Comp Neurol* 203:595–612.
- Reiner A, Karten HJ. 1978. A bisynaptic retinocerebellar pathway in the turtle. *Brain Res* 150:163–169.
- Ruberstone JA, Mehler WR, Voogd J. 1995. The vestibular nuclear complex. In: Paxinos G, editor. *The rat nervous system*. 2nd ed. Sydney: Academic Press. p 773–796.
- Ruigrok TJH, Osse RJ, Voogd J. 1992. Organization of inferior olivary projections to the flocculus and ventral paraflocculus of the rat cerebellum. *J Comp Neurol* 316:129–150.
- Sato Y, Kanda K-I, Kawasaki T. 1987. Target neurons of floccular middle zone inhibition in medial vestibular nucleus. *Brain Res* 446:225–235.
- Simpson JI. 1984. The accessory optic system. *Annu Rev Neurosci* 7:13–41.
- Simpson JI, Graf W, Leonard CS. 1981. The coordinate system of visual climbing fibres to the flocculus. In: Fuchs AF, Becker W, editors. *Progress in oculomotor research*. Amsterdam: Elsevier. p 475–484.
- Simpson JI, Leonard CS, Soodak RE. 1988. The accessory optic system: analyzer of self-motion. *Ann N Y Acad Sci* 545:170–179.
- Simpson JI, Graf W, Leonard CS. 1989a. Three-dimensional representation of retinal image movement by climbing fiber activity. In: Strata P, editor. *The olivocerebellar system in motor control. Experimental brain research: supplement. Volume 17*. Heidelberg: Springer-Verlag. p 323–327.
- Simpson JI, Van der Steen J, Tan J, Graf W, Leonard CS. 1989b. Representations of ocular rotations in the cerebellar flocculus of the rabbit. In: Allum JHJ, Hulliger M, editors. *Progress in brain research. Volume 80*. Amsterdam: Elsevier. p 213–223.
- Takeda T, Maekawa K. 1976. The origin of the pretecto-olivary tract. A study using horseradish peroxidase. *Brain Res* 117:319–325.
- Takeda T, Maekawa K. 1989a. Olivary branching to the flocculus, nodulus and ventral uvula in the rabbit. I. An electrophysiological study. *Exp Brain Res* 74:47–62.
- Takeda T, Maekawa K. 1989b. Olivary branching to the flocculus, nodulus and ventral uvula in the rabbit. II. Retrograde double labeling study with fluorescent dyes. *Exp Brain Res* 76:323–332.
- Tan J, Gerrits NM, Nanhoe RS, Simpson JI, Voogd J. 1995a. Zonal organization of the climbing fibre projection to the flocculus and nodulus of the rabbit. A combined axonal tracing and acetylcholinesterase histochemical study. *J Comp Neurol* 356:23–50.
- Tan J, Epema AH, Voogd J. 1995b. Zonal organization of the flocculo-vestibular nucleus projection in the rabbit. A combined axonal tracing and acetylcholinesterase histochemical study. *J Comp Neurol* 356:51–71.
- Veenman CL, Reiner A, Honig MG. 1992. Biotinylated Dextran amine as an anterograde tracer for single- and double-labeling studies. *J Neurosci Methods* 41:239–254.
- Wild JM. 1993. Descending projections of the songbird nucleus robustus archistrialis. *J Comp Neurol* 338:225–241.
- Winfield JA, Hendrickson A, Kimm J. 1978. Anatomical evidence that the

- medial terminal nucleus of the accessory optic tract in mammals provides a visual mossy fiber input to the flocculus. *Brain Res* 151:175–182.
- Winship IR, Wylie DRW. 2001. Responses of neurons in the medial column of the inferior olive in pigeons to translational and rotational optic flowfields. *Exp Brain Res* 141:63–78.
- Winship IR, Wylie DRW. 2003. Zonal organization of the vestibulocerebellum in pigeons (*Columba livia*): I. Climbing fiber input to the flocculus. *J Comp Neurol* 456:127–139.
- Wold JE. 1976. The vestibular nuclei in the domestic hen (*Gallus domesticus*). I. Normal anatomy. *Anat Embryol* 149:29–46.
- Wylie DRW. 2001. Projections from the nucleus of the basal optic root and nucleus lentiformis mesencephali to the inferior olive in pigeons (*Columba livia*). *J Comp Neurol* 429:502–513.
- Wylie DR, Frost BJ. 1993. Responses of pigeon vestibulocerebellar neurons to optokinetic stimulation: II. The 3-dimensional reference frame of rotation neurons in the flocculus. *J Neurophysiol* 70:2647–2659.
- Wylie DRW, Frost BJ. 1996. The pigeon optokinetic system: visual input in extraocular muscle coordinates. *Vis Neurosci* 13:945–953.
- Wylie DRW, Frost BJ. 1999. Complex spike activity of Purkinje cells in the ventral uvula and nodulus of pigeons in response to translational optic flowfields. *J Neurophysiol* 81:256–266.
- Wylie DR, Kripalani T-K, Frost BJ. 1993. Responses of pigeon vestibulocerebellar neurons to optokinetic stimulation: I. Functional organization of neurons discriminating between translational and rotational visual flow. *J Neurophysiol* 70:2632–2646.
- Wylie DRW, Linkenhoker B, Lau KL. 1997. Projections of the nucleus of the basal optic root in pigeons (*Columba livia*) revealed with biotinylated dextran amine. *J Comp Neurol* 384:517–536.
- Wylie DRW, Bischof WF, Frost BJ. 1998. Common reference frame for neural coding of translational and rotational optic flow. *Nature* 392:278–282.
- Wylie DRW, Lau KL Jr, Lu X, Glover RG, Valsangkar-Smyth M. 1999a. Projections of Purkinje cells in the translation and rotation zones of the vestibulocerebellum in pigeon (*Columba livia*). *J Comp Neurol* 413:480–493.
- Wylie DRW, Winship IR, Glover RG. 1999b. Projections from the medial column of the inferior olive to different classes of rotation-sensitive Purkinje cells in the flocculus of pigeons. *Neurosci Lett* 268:97–100.
- Yamamoto M. 1978. Localization of rabbit's flocculus Purkinje cells projecting to the lateral cerebellar nucleus and the nucleus prepositus hypoglossi investigated by means of retrograde transport of horseradish peroxidase. *Neurosci Lett* 7:97–202.